

Effect of post-annealing on martensitic transformation and magnetocaloric effect in $\text{Ni}_{45}\text{Co}_5\text{Mn}_{36.7}\text{In}_{13.3}$ alloys

L. Chen,^{1,2} F. X. Hu,^{1,a)} J. Wang,¹ J. Shen,¹ J. R. Sun,¹ B. G. Shen,¹ J. H. Yin,² L. Q. Pan,² and Q. Z. Huang³

¹State Key Laboratory of Magnetism, Institute of Physics, Chinese Academy of Sciences, Beijing 100190, People's Republic of China

²Department of Physics, University of Science and Technology Beijing, Beijing 100083, People's Republic of China

³NIST Center for Neutron Research, National Institute of Standards and Technology, Gaithersburg, Maryland 20899, USA

(Presented 16 November 2010; received 23 September 2010; accepted 22 December 2010; published online 8 April 2011)

The metamagnetic alloy $\text{Ni}_{45}\text{Co}_5\text{Mn}_{36.7}\text{In}_{13.3}$ was fabricated by conventional arc-melting technique. Subsequent annealing may relax the stress and modify the atom ordering, thus influencing the magnetic properties and martensitic transformation behaviors. Our studies demonstrate that post-annealing at temperatures $\leq 300^\circ\text{C}$ can lead to a significant change in the magnetic properties and martensitic temperature (T_M). Annealing the sample at 300°C for 3 h can cause a decrease of as much as 30 K in T_M (from 319 to 289 K) while retaining strong metamagnetic behaviors. The field-induced metamagnetic transition is accompanied with a large magnetocaloric effect. With an increase in the annealing temperature, the magnitude of the effective magnetic entropy change decreases somewhat, while the refrigeration capacity shows a slight increase. © 2011 American Institute of Physics. [doi:10.1063/1.3565189]

Recently, increasing attention has been paid to the magnetic refrigeration technique, which is based on the magnetocaloric effect (MCE). People have discovered many kinds of materials that show great MCE, particularly the ones with first-order transitions.^{1–4} Among those materials, an attractive candidate is Mn-based Heusler alloy.^{5–8} The recent discovery of metamagnetic shape memory alloys has stirred intense interest because of their huge shape memory effects and different mechanism compared to the conventional FSMAs. In G-free metamagnetic Ni–Mn–Z alloys (where Z can be a group III or group IV element such as In, Sn, or Sb),⁹ the strong change of magnetization across the martensitic transformation results in a large Zeeman energy $\mu_0\Delta M \cdot H$, which drives the structural transformation and causes field-induced metamagnetic behavior. Furthermore, the incorporation of Co into these alloys enlarges the magnetization difference across the martensitic transformation and enhances the Zeeman energy $\mu_0\Delta M \cdot H$, thus resulting in an extremely huge ferromagnetic shape memory effect.^{10,11}

The fundamental changes in magnetic properties, electronic structure, and scattering mechanism during the metamagnetic process result in a large MCE and a distinct magnetoresistance (MR) effect. In order to realize these novel functions in a wide temperature range, people are eager to find ways of tuning T_M arbitrarily while retaining strong metamagnetic properties. Normally, the method to tune T_M is to adjust the valence electron concentration (e/a) by changing compositions or introducing other elements.

Here, we report a different way to tune T_M by post-annealing. The as-prepared samples may contain stress because they were quenched from 1173 K to ice-water temperature at the end of their preparation. Subsequent annealing can relax the stress and modify the atom site/order, the Mn–Mn distance, and the lattice symmetry.^{12,13} As a result, the Mn–Mn exchange coupling, the Brillouin zone boundary, and, thus, T_M might be changed. Our studies indicate that post-annealing at temperatures $\leq 300^\circ\text{C}$ can move T_M to lower temperatures while retaining strong metamagnetic properties. By simply modulating the annealing temperature and duration, T_M can be tunable in a wide temperature range, and a large MCE takes place in an extended temperature range near room temperature.

We prepared $\text{Ni}_{45}\text{Co}_5\text{Mn}_{50-x}\text{In}_x$ ($x = 13.3, 13.5$) alloys in one batch by arc-melting technique.¹⁰ The ingots were homogenized at 1173 K for 24 h and then quenched in ice water. Small pieces were cut from the ingots and annealed at 250°C (250°C -annealed sample) or 300°C (300°C -annealed sample) for 3 h and then quenched in ice water. All magnetic measurements were carried out using a Quantum Design MPMS-7 superconducting quantum interference device magnetometer. High-resolution powder-diffraction data were collected at the NIST Center for Neutron Research on the BT-1 high-resolution neutron powder diffractometer, using monochromatic neutrons of wavelength 1.1968 \AA produced by a Ge(733) monochromator.

To be aware of the chemical ordering of the parent phase for the as-prepared samples, we chose $\text{Ni}_{45}\text{Co}_5\text{Mn}_{36.5}\text{In}_{13.5}$ (martensitic transition temperature $T_M \sim 280 \text{ K}$, determined from magnetothermal experiments) and performed neutron diffraction measurements at room temperature [Fig. 1(a)].

^{a)}Author to whom correspondence should be addressed. Electronic mail: hufox@g203.iphy.ac.cn.

Rietveld refinements revealed that the main austenitic phase coexists with a 34% martensitic phase at room temperature due to a T_M close to room temperature. The austenitic phase appears in the $L2_1$ -type order structure (space group: $Fm-3m$) [see the details in the inset of Fig. 1(a)], whereas the martensitic phase is in the body-centered tetragonal (bct; space group: $I4/mmm$) structure; note the appearance of characteristic peaks (111), (311) of $L2_1$ -type order.

Figure 1(b) exhibits XRD patterns of as-prepared and 300 °C-annealed samples for another composition, $Ni_{45}Co_5Mn_{36.7}In_{13.3}$, collected at room temperature. T_M appears at 319 K [see Fig. 2] for the as-prepared sample, and shifts to 289 K (still not far from room temperature) upon additional annealing at 300 °C for 3 h [see Fig. 2]. So, the XRD patterns for both the as-prepared and the 300 °C-annealed samples show the coexistence of austenitic and martensitic phases, which was also identified to be of $L2_1$ -type order and bct structure.

There are several reported methods to characterize order degree. ^{14–16} According to the simplest and most classical method, ^{14,15} S_H , the degree of the $L2_1$ -type order, can be determined from the XRD intensity ratio of the superlattice and the fundamental reflections $I(111)/I(220)$ in the following way:

$$S_H^2 = [I(111)/I(220)]_{exp} / [I(111)/I(220)]_{cal},$$

where I is the peak intensity of the x-ray diffraction and the notations “exp” and “cal” mean “experimental” and “calculation,” respectively.

The calculated intensity ratio of $[I(111)/I(220)]_{cal}$ is crucially dependent on the atomic occupations. We assumed all

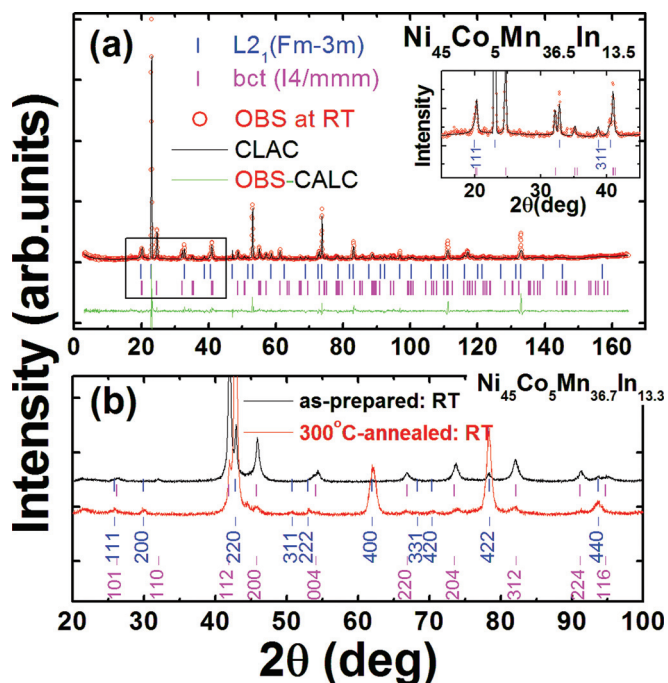


FIG. 1. (Color online) (a) Observed (OBS) and calculated (CALC) intensities for neutron diffraction data collected at room temperature (RT) [wavelength 1.1968 Å by a Ge(733) monochromator] for $Ni_{45}Co_5Mn_{36.5}In_{13.5}$. (b) XRD patterns of the as-prepared and 300 °C-annealed samples for $Ni_{45}Co_5Mn_{36.7}In_{13.3}$ collected at room temperature (RT).

Co atoms occupy Ni positions and the rest of the Mn atoms ($36.7-25$ in $Ni_{45}Co_5Mn_{36.7}In_{13.3}$) occupy In positions, and then calculated the order degree of our samples. We found that the obtained S_H of the $L2_1$ order is 0.86 and 0.77 for the as-prepared and 300 °C-annealed $Ni_{45}Co_5Mn_{36.7}In_{13.3}$, respectively. One can see that the degree of the $L2_1$ order is getting smaller with low temperature annealing.

Figure 2 displays the temperature dependent zero-field-cooled (ZFC) and field-cooled (FC) magnetization measured under different fields of 0.02 T and 5 T for $Ni_{45}Co_5Mn_{36.7}In_{13.3}$ samples. With subsequent annealing of the sample at 250 °C and 300 °C for 3 h, the martensitic transition temperature, T_M , gradually shifts to lower temperatures. T_M under 0.02 T appears at 319, 300, and 289 K (here, T_M is defined following the rule used in Ref. 10 and indicated in Fig. 2), and the corresponding temperature hysteresis is 12, 14, and 14 K for the as-prepared, 250 °C-annealed, and 300 °C-annealed $Ni_{45}Co_5Mn_{36.7}In_{13.3}$ samples, respectively (see Table I). The shift in T_M can be as large as 30 K when the sample is annealed at 300 °C for 3 h, while a slight widening of the hysteresis gap appears for the annealed samples. One can notice that the magnetization change (ΔM) across the martensitic transformation under 5 T is about the same (~ 100 emu/g) for the three samples. Such a large ΔM results in a large Zeeman energy, $\mu_0 \Delta M \cdot H$, which pushes T_M to lower temperatures at a rate of 4.0, 5.4, and 6.8 K/T, respectively. It was found that T_M under 5 T locates at 299, 273, and 255 K for the as-prepared, 250 °C-annealed, and 300 °C-annealed samples, respectively (see Table I). The driving rate of T_M by a magnetic field does not drop, but it shows a small increase upon annealing. These results demonstrate that the annealed samples still retain strong metamagnetic properties. Thus, a large MCE is expected even for the annealed samples.

Modifying the e/a is a common way to adjust T_M . However, besides the effect of e/a on T_M , many other factors, such as stress distribution at phase boundaries and atomic ordering, ¹² can also affect T_M . The stress formed during the quenching process was relaxed to some extent depending on the additional annealing temperature and duration, which

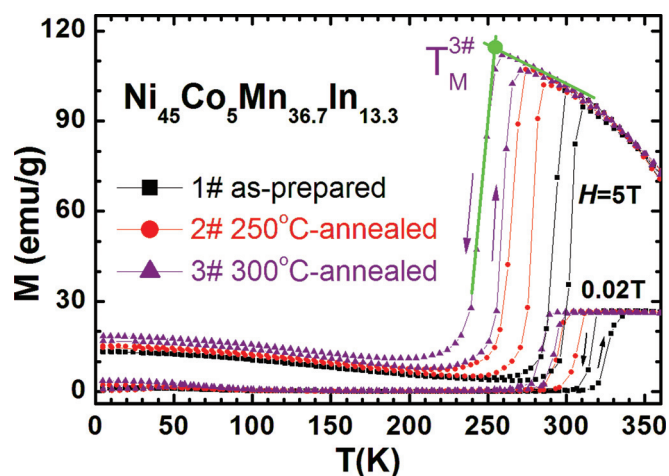


FIG. 2. (Color online) The temperature dependence of zero-field-cooled and field-cooled magnetization (M - T curve) under different fields of 0.02 T and 5 T for the as-prepared, 250 °C-annealed, and 300 °C-annealed $Ni_{45}Co_5Mn_{36.7}In_{13.3}$ samples. The arrows indicate the heating/cooling path.

TABLE I. Martensitic temperature under 0.02 T ($T_{M, 0.02 T}$) and 5 T ($T_{M, 5 T}$), driving rate of the magnetic field on T_M , thermal hysteresis under 0.02 T, effective magnetic entropy change ($\Delta S_{\text{effective}}$) and its half-peak width (ΔT_M), and refrigeration capacity (RC) for the as-prepared, 250 °C-annealed, and 300 °C-annealed $\text{Ni}_{45}\text{Co}_5\text{Mn}_{36.7}\text{In}_{13.3}$ samples.

Samples	$T_{M, 0.02 T}$ (K)	$T_{M, 5 T}$ (K)	Driving rate of T_M (K/T)	Thermal hysteresis (K)	$\Delta S_{\text{effective}}$ ($\text{J kg}^{-1}\text{K}^{-1}$)	ΔT_M (K)	RC (J kg^{-1})
As-prepared	319	299	4.0	12	~ 20	20	295
250 °C-annealed	300	273	5.4	14	~ 17	27	333
300 °C-annealed	289	255	6.8	14	~ 15	34	350

may modify atom site/ordering,^{12,13} Mn–Mn distance, and lattice symmetry. As a result, the Mn–Mn exchange coupling, Fermi surface, and Brillouin zone boundary can be changed.^{17–19} All these combined elements result in a change of martensitic transformation, leading to a decrease in T_M .

Figure 3 displays the magnetic entropy change (ΔS) as a function of temperature under a magnetic field of 5 T calculated using the Maxwell relation,^{1–4} $\Delta S(T, H) = S(T, H) - S(T, 0) = \int_0^H (\partial M / \partial T) H^{\text{dH}}$. The maximum ΔS peak reaches $\sim 38 \text{ J kg}^{-1}\text{K}^{-1}$, $\sim 32 \text{ J kg}^{-1}\text{K}^{-1}$, and $\sim 31 \text{ J kg}^{-1}\text{K}^{-1}$ for the as-prepared, 250 °C-annealed, and 300 °C-annealed samples, respectively. However, how to accurately calculate ΔS in a first-order system has remained a controversial question for a quite a long time. Recent investigations indicated that ΔS can be seriously overestimated for a nonequilibrium/multiphase coexistent system by using the Maxwell relation.^{20–22} In these systems, the ΔS peak usually exhibits an extremely high spike followed by a plateau. Detailed studies suggested that such an extremely high ΔS spike comes from the overrating of ΔS due to the coexistence of two phases at temperatures very close to the transition point. However, our careful investigations based on specific heat measurements verified that the ΔS plateau at temperatures away from transition point does reflect the intrinsic nature of ΔS .²² Accordingly, the ΔS plateau height is about 20, 17, and 15 J/kgK, and the corresponding half-peak width (ΔT_M) is 20 K,

27 K, and 34 K, for the as-prepared, 250 °C-annealed, and 300 °C-annealed samples, respectively (see Table I). As is known, refrigerant capacity (RC) is another key parameter in the estimation of MCE, which is defined as²³

$$\text{RC} = \int_{T_1}^{T_2} \Delta S(T)_H dT,$$

where T_1 and T_2 are the temperatures of the cold and hot reservoirs of the refrigeration cycle, respectively. According to the method available from the literature,²³ the value of RC can be obtained by performing the integration over the full width at half maximum in a ΔS – T curve. The obtained RC value under 5 T reaches 295 J kg^{-1} , 333 J kg^{-1} and 350 J kg^{-1} for the as-prepared, 250 °C-annealed, and 300 °C-annealed samples, respectively (see Table I and patterned areas in Fig. 3). One can notice that the effective ΔS magnitude decreases somewhat, whereas RC shows a slight increase with increasing annealing temperature for the present composition $\text{Ni}_{45}\text{Co}_5\text{Mn}_{36.7}\text{In}_{13.3}$.

This work was supported by the National Natural Science Foundation of China, the Knowledge Innovation Project of the Chinese Academy of Sciences, and the Hi-Tech Research and Development Program of China. The authors also gratefully acknowledge the support of K. C. Wong Education Foundation, Hong Kong.

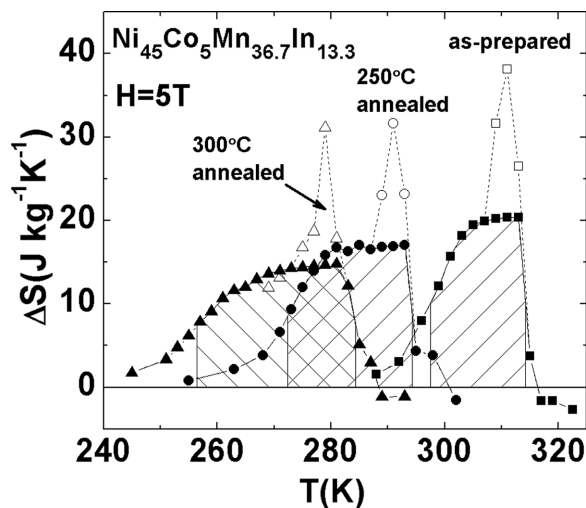


FIG. 3. Magnetic entropy change ΔS as a function of temperature under a magnetic field of 5 T calculated using the Maxwell relation for the as-prepared, 250 °C-annealed, and 300 °C-annealed $\text{Ni}_{45}\text{Co}_5\text{Mn}_{36.7}\text{In}_{13.3}$ samples. The solid line and the patterned areas correspond to the effective ΔS and the refrigeration capacity, respectively.

¹A. M. Tishin and Y. I. Spichkin, *The Magnetocaloric Effect and Its Applications* (Institute of Physics, Bristol, 2003).

²K. A. Gschneidner, Jr. *et al.*, *Rep. Prog. Phys.* **68**, 1479 (2005).

³E. Bruck, in *Handbook of Magnetic Materials*, edited by K. H. J. Buschow (North-Holland, Amsterdam, 2008), Vol. 17.

⁴B. G. Shen *et al.*, *Adv. Mater.* **21**, 4545 (2009).

⁵F. X. Hu *et al.*, *Appl. Phys. Lett.* **76**, 3460 (2000).

⁶F. X. Hu *et al.*, *Phys. Rev. B* **64**, 132412 (2001).

⁷J. Marcos *et al.*, *Phys. Rev. B* **68**, 094401 (2003).

⁸S. Stadler *et al.*, *Appl. Phys. Lett.* **88**, 192511 (2006).

⁹Y. Sutou *et al.*, *Appl. Phys. Lett.* **85**, 4358 (2004).

¹⁰R. Kainuma *et al.*, *Nature* **439**, 957 (2006).

¹¹H. E. Karaca *et al.*, *Adv. Funct. Mater.* **19**, 983 (2009).

¹²W. Ito *et al.*, *Appl. Phys. Lett.* **93**, 232503 (2008); *ibid.* **92**, 021908 (2008).

¹³S. Kustov *et al.*, *Appl. Phys. Lett.* **94**, 191901 (2009).

¹⁴L. Muldrew, *J. Appl. Phys.* **37**, 2062 (1966).

¹⁵Y. Murakami *et al.*, *Trans. Jpn. Inst. Met.* **21**, 708 (1980).

¹⁶Y. Takamura *et al.*, *J. Appl. Phys.* **105**, 07B109 (2009).

¹⁷P. J. Webster *et al.*, *Philos. Mag. B* **49**, 295 (1984).

¹⁸P. Entel *et al.*, *J. Phys. D: Appl. Phys.* **39**, 865 (2006).

¹⁹H. Sato and R. S. Toth, *Phys. Rev.* **124**, 1833 (1961).

²⁰J. S. Amaral and V. S. Amaral, *Appl. Phys. Lett.* **94**, 042506 (2009).

²¹M. Balli *et al.*, *Appl. Phys. Lett.* **95**, 072509 (2009).

²²G. J. Liu *et al.*, *Appl. Phys. Lett.* **90**, 032507 (2007).

²³D. L. Schlögl *et al.*, *Scr. Mater.* **59**, 1083 (2008).